

PHYSICS

Neuronal Ensembles with Balanced Interconnection as Receptors of Information

A. K. Kozlov*, R. Huerta**, Corresponding Member of the RAS M. I. Rabinovich*,
H. D. I. Abarbanel**, and M. V. Bazhenov*

Received July 1, 1997

Comprehensive anatomical and physiological experiments of the last ten to fifteen years aimed at getting insight into the nervous system have made it possible to identify certain basic neuronal structures (the basic neural circuits) that serve as building blocks for more complex (large and small) nervous systems. Such basic neural circuits commonly occur in vertebrates and invertebrates alike [1, 2]. The elements of these structures can be either isolated neuronal generators or large neuron ensembles that generate, for example, short-impulse bursts (impulse spikes). The architecture of basic neuronal structures is governed by the types of interconnections between the elements. As a rule, these are synaptic (exciting or inhibiting) interconnections. Electrical interconnections between neurons are also typical of many neuronal structures and are determined by diffusion within a small gap between the presynaptic and postsynaptic membranes [3, 4]. Judging from all the evidence, it is difficult to recognize any first principles in the construction of neuronal structures. Nevertheless, analysis of various basic networks makes it possible to isolate certain universal techniques employed by nature in constructing these networks. One such technique, it seems to us, would be a simultaneous implementation of antagonistic interconnections that, in a sense, compensate each other. The antagonism of the interconnections can manifest itself in a rich variety of ways. However, if we are concerned with neuronal oscillators, we can state that a synaptic exciting interconnection tends to synchronize the activity of neurons [5, 6]. As for the inhibiting interconnection, it is responsible for antiphase oscillations as a rule [6–8]. Electrical interconnection also typically synchronizes the neurons [5, 9] much as the random-impulse generators are synchronized in radio engineering [10]. In many nervous systems, such antagonistic interconnec-

tions operate in parallel. For example, in central pacemaking generators, parallel inhibiting and electrical interconnections [3, 11] (chain I in Fig. 1) and parallel inhibiting and exciting interconnections (chains II and III) are encountered. A similar pattern is observed also in many of the basic neuronal networks of the brain. It is noteworthy that, in the diagrams shown in Fig. 1, each of the subsystems I and 2 can represent either a single neuron or an ensemble of synchronized neurons. In small neuronal systems like the pacemaking generators, the compensation of antagonistic interconnections (i.e., a balance) is achieved by equalizing the magnitude of the coupling, which results in compensation of oppositely acting synaptic currents. In the case of large neuronal ensembles, attainment of a balance can also be controlled by varying the number of interconnections (e.g., exciting and inhibiting).

Why has evolution retained the parallel-acting antagonistic interconnections? The answer to this and similar questions requires at least the development of adequate dynamic models for neuronal structures with balanced interconnections and the analysis of behavior of these structures under the effects of external signals (i.e., under the effects of stimuli). This is the problem

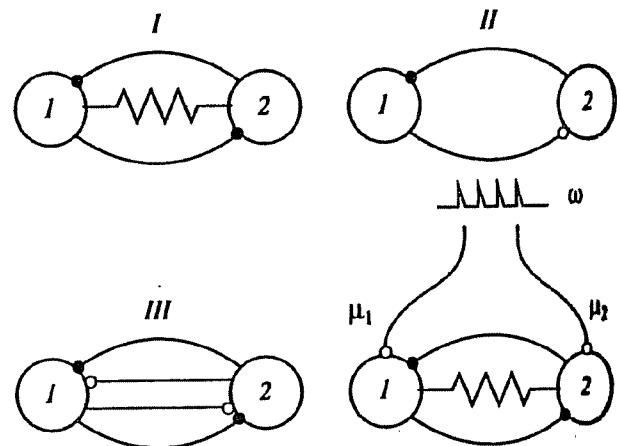


Fig. 1. Basic neuronal chains.

* Institute of Applied Physics,
Russian Academy of Sciences,
ul. Ul'yanova 46, Nizhnii Novgorod, 603600 Russia

** Institute for Nonlinear Science, University of California,
San Diego, La Jolla, CA 92093-0402, USA

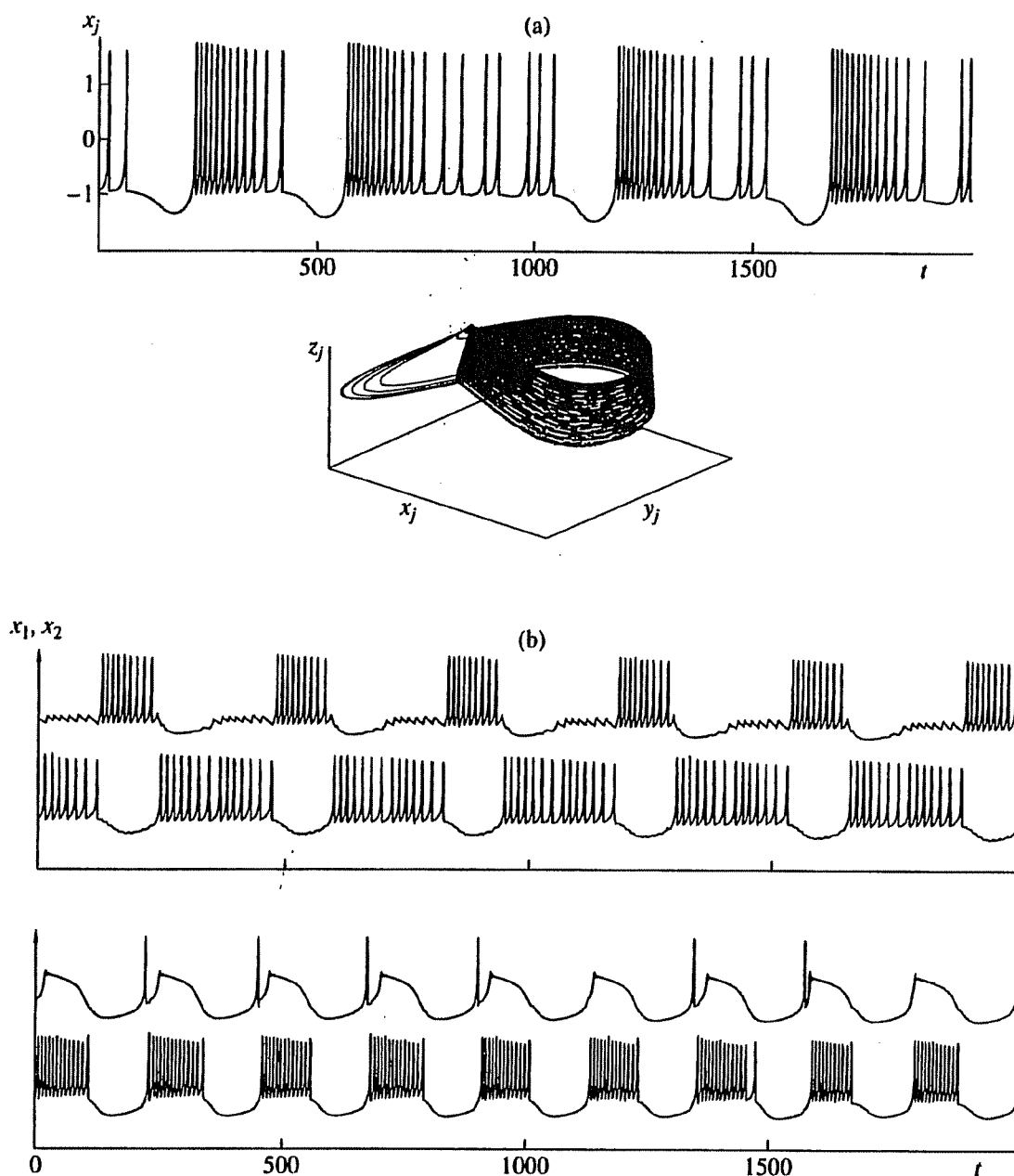


Fig. 2. Self-governing dynamics of chains: (a) realization and an attractor in the model of isolated neuron; (b) inphase and antiphase oscillations in chain II; (c) hysteresis and bistability in chain I; and (d) hysteresis and bistability in chain III.

to be solved in this study. We investigate the functional role of balanced interconnection in the context of a minimal neuronal chain consisting of two linked identical subsystems. It is assumed that each subsystem constitutes an oscillator with chaotic pulse-burst activity. Such activity is characteristic of the individual dynamics of various live neurons, for example, of the neurons involved in the central pyloric-pacemaker of lobsters [3, 11]. In order to analyze the cooperative behavior of basic neuronal chains, we will utilize the well-known Hindmarsh-Rose model [12], which describes the generation of impulse bursts (spikes), and

add to this model the expressions characterizing the interconnections. As a result, we have

$$\begin{aligned} \frac{dx_j}{dt} &= ax_j^2 - bx_j^3 + y_j - z_j + I - E_{jk} - S_{jk} + \mu_j \alpha(t), \\ \frac{dy_j}{dt} &= c - dx_j^2 - y_j, \quad \frac{dz_j}{dt} = r[s(x_j - x_0) - z_j], \end{aligned} \tag{1}$$

with $j = 1, 2$ and $k = 2, 1$ ($k \neq j$).

Here, x_j is the membrane potential of the j th neuron, y_j is the generalized variable that describes the ionic

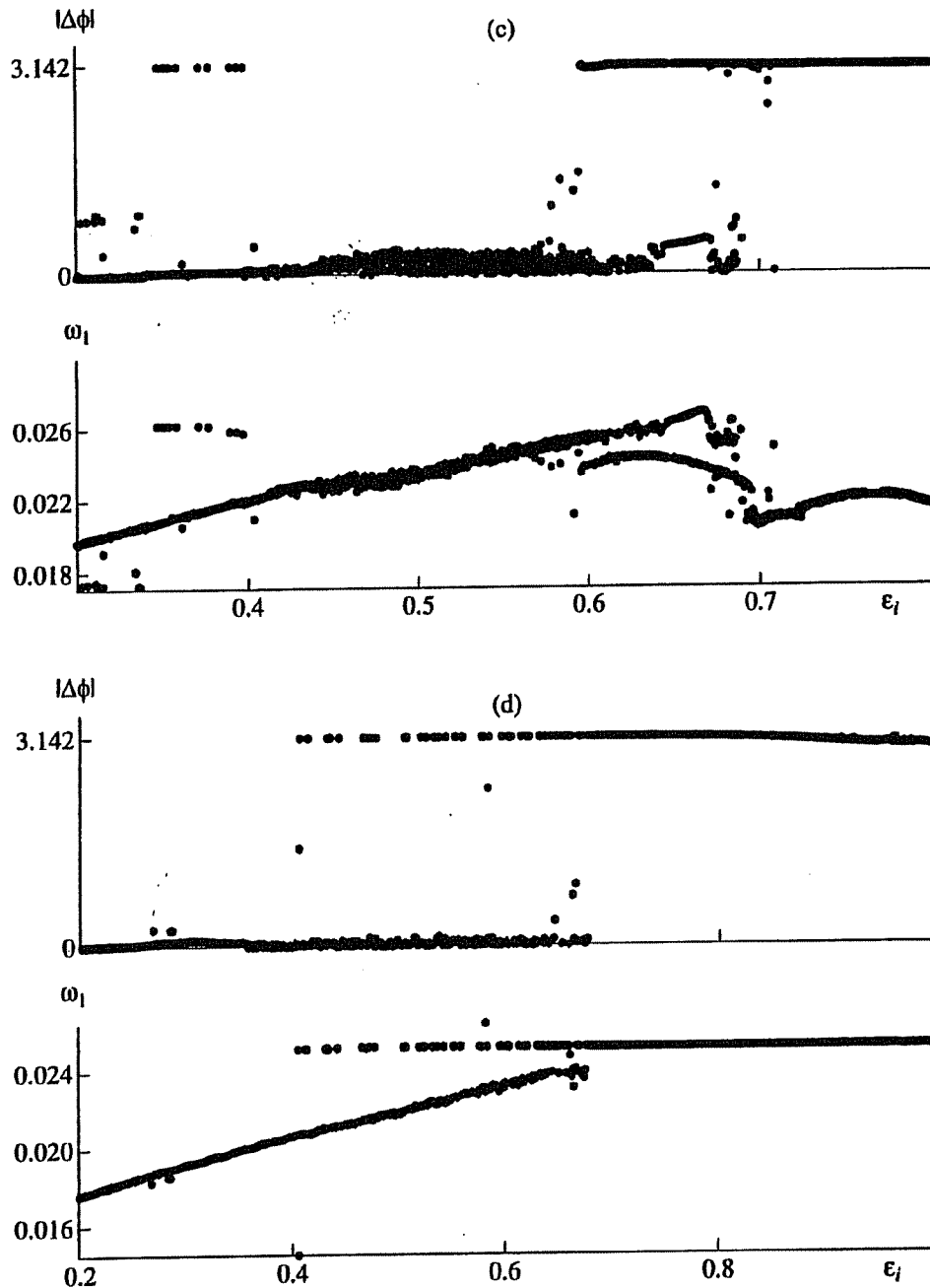


Fig. 2. (Contd.)

currents responsible for the spike generation (in particular, the currents of K^+ and Na^+), and the variable z_j characterizes the slow processes (in particular, variations in the Ca^{++} -ion concentration). The terms E_{jk} and S_{jk} define the interconnections between the neurons, and the external force $\mu_j \alpha(t)$ [$\max \alpha(t) = 1$] is represented by the train of positive impulses of amplitude μ_j , which simulate the effect of the stimulus. The values of the parameters of each of the simulated neurons are assumed to be specified as

$$\begin{aligned} a = 3, \quad b = 1, \quad c = 1, \quad d = 5, \\ r = 0.0021, \quad s = 4, \quad x_0 = -1.6. \end{aligned} \quad (2)$$

The external current I defines the characteristic generation period for the bursts and also the type of oscillations. In particular, with $I = 3.281$ and the values of the parameters given by (2), a self-contained neuron exhibits a chaotic behavior. The oscilloscope pattern $x_j(t)$ of this process and the corresponding phase trajectory in the space (x_j, y_j, z_j) are shown in Fig. 2a.

In all the situations under consideration, system (1) was solved numerically with the use of the explicit Dormann-Prince scheme of the order 5(4) with a local error of 10^{-8} .

Let us consider the dynamics of self-contained chains ($\mu_1 = \mu_2 = 0$) as a function of the type of interconnection between neurons. The interconnection in basic chains I, II, and III (as shown in Fig. 1) is realized via the perturbations of membrane current and is provided either by diffusion [i.e., electrically, as specified by $E_{jk} = \epsilon_e(x_j - x_k)$] or with the use of chemical synapses $S_{jk} = \epsilon_j(x_j + V_j)F(x_k - X_j) + \dots$. The interconnection function has the sigmoidal form

$$F(w) = \frac{1}{1 + \exp(-w/T)}, \quad T = 0.01.$$

With $V_j = 0$, the chemical interconnection is exciting, and, with $V_j = 1.4$, it is inhibiting. The magnitudes of threshold potentials in chains I and II are regarded as the same for all interconnections ($X_1 = X_2 = -0.85$); in chain III, these potentials are assumed to depend on whether the interconnection is exciting or inhibiting ($X_1^{inh} = X_2^{inh} = -0.85$ and $X_1^{exc} = X_2^{exc} = -0.7$).

Sufficiently strong electrical or exciting interconnections present in system (1) result in the inphase synchronization of interacting neurons [6]. In this case, an entire network behaves as a single neuron. By contrast, a strong inhibiting interconnection provides an antiphase synchronization; i.e., the periods of neuronal activity during which the spikes can be generated alternate. Examples of the inphase and antiphase behavior of neurons are illustrated in Fig. 2b.

The introduction of antagonistic interconnection into a neuron pair radically changes the dynamics and functionality of the pair. Common to chains I, II, and III is the existence of oscillations of one of the fundamental modes (e.g., inphase or antiphase) in the parameter space corresponding to the stability domain; a transition region (where the interconnections are mutually compensated and a rather complex dynamics is observed in the system) is also common to these chains. When the coupling magnitude is varied and the transition region is passed, the oscillations of the subsystems transform from inphase into antiphase, and vice versa. However, this occurs dissimilarly for chains of different types.

In the chains with symmetric interconnections, i.e., inhibiting and electrical (chain I features $I = 3.281$, $\epsilon_e = 0.1$, $0 < \epsilon_i < 1$, and $\epsilon_i = \epsilon_1 = \epsilon_2$) and also inhibiting and exciting (chain III features $I = 2.5$, $\epsilon_{1,2}^{exc} = 0.2$, $0 < \epsilon_i < 1$, and $\epsilon_i = \epsilon_1^{inh} = \epsilon_2^{inh}$), a hysteresis is observed in the transition region and is related to bistability (or multistability, for certain values of the parameters). Bistability manifests itself in the coexistence of modes that have markedly different average phase shifts between the periods of activity of interacting neurons.

As is evident from Figs. 2c and 2d, two fundamental modes of oscillations are realized in chain I for $\epsilon_e = 0.1$ and in chain III for $\epsilon_1^{exc} = \epsilon_2^{exc} = 0.2$ (and for different values of ϵ_i); one of the modes features a small phase shift for bursts (the inphase oscillations) and the other mode has an average oscillation-phase shift close to π (the antiphase oscillations). It is evident from Figs. 2c and 2d that different average burst rates are characteristic of the modes of inphase and antiphase oscillations that are observed in the bistability domain; the upper branch in the diagram for $\omega_1(\epsilon_i)$ corresponds to inphase oscillations for chain I and the lower branch corresponds to antiphase oscillations (the situation is the reverse for chain III).

In the transition region, neurons are desynchronized, and chaotic oscillations become set in system (1) in the case of asymmetric chain II with exciting and inhibiting interconnections for $V_1 = 1.4$, $V_2 = 0$, $0 < \epsilon_1 < 1$, and $\epsilon_2 = 0.2$.

Special features of self-governing dynamics of the neuronal oscillators under consideration define also the response of these oscillators to an input signal, i.e., a stimulus. We studied the results of exposing such oscillators to relatively short-term (with the characteristic time equal to about 10 bursts of activity) external stimulation in the form of a pulse train given by

$$\alpha(t) = C_0(t - t_n) \exp\left(-\frac{t - t_n}{T_a}\right),$$

where t_n are the instants of time corresponding to the delivery of pulses, $T_a = 20$, and C_0 is a normalization multiplier. Such a signal was fed to both simulated neurons from each chain as shown in Fig. 1 for chain I. We studied most comprehensively the non-self-governing dynamics of the neuron pair in the transition region of parameters where, in the absence of external stimulus, mutual compensation of interconnections resulted in bistability or chaos. The results of the simulation are illustrated in Figs. 3 and 4. As is evident, the behavior of neuron pairs is extremely sensitive to the spike-to-spike time interval in the input signal. It was found that the effect of small-amplitude burst-like stimulus with repetition rate of the pulses in the burst chosen close to the levels of one or another branch $\omega_1(\epsilon_i)$ in Figs. 2c or 2d can cause a transition from inphase oscillations to antiphase ones and vice versa. An example of such transitions in chain I with $\epsilon_e = 0.1$ and $\epsilon_i = 0.65$ is shown in Fig. 3. Chain III with $\epsilon_1^{exc} = \epsilon_2^{exc} = 0.2$ and $\epsilon_i = 0.65$ demonstrates similar behavior. Thus, it is possible to recognize and store information about the spike-to-spike time interval in chains with bistability.

As is evident from Fig. 4, chain II with asymmetric interconnections is also able to discern stimuli with different spike rates because this chain undergoes the transition from chaos to inphase oscillations at a certain rate of the stimulating spikes. Such behavior may be

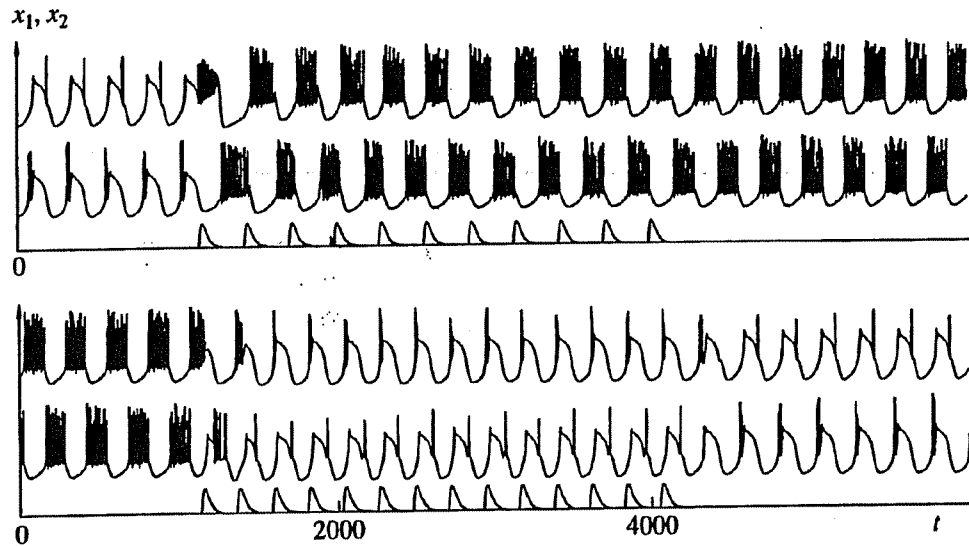


Fig. 3. Recognition and storage of information by chains featuring bistability.

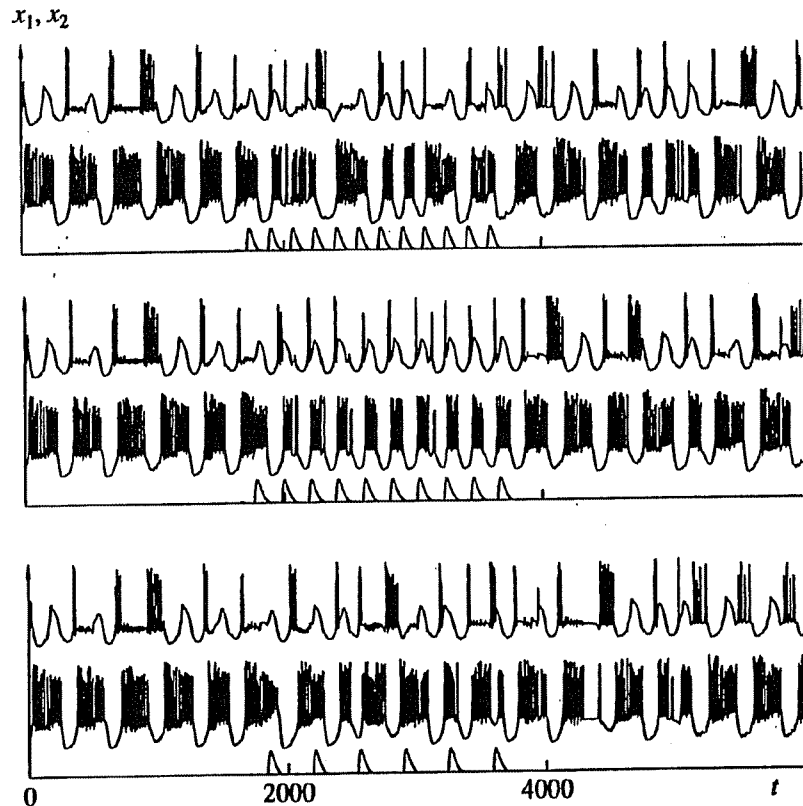


Fig. 4. Recognition of a signal by chain II.

correlated with the function of the indicator (or detector), which picks out information signals from the general signal flow. It is also worth noting that the absence of a stable regime in a self-contained system in the case of chain II does not permit the preservation of the response form when stimulation is terminated, so that

information on the input signal becomes lost; the farther the interconnection parameters (the patterns in Fig. 4 are computed for $\epsilon_1 = 0.85$, which corresponds to the central part of transition region) are chosen from the synchronization threshold in the transition region, the more rapidly the loss of information occurs.

Thus, the minimum-size neuronal systems (the pairs of identical neurons) with balanced coupling in the form of parallel-acting antagonistic interconnections (inhibiting and electrical or inhibiting and exciting) exhibit the following functional characteristics: (i) a large number of scenarios of stable behavior of the system owing to the dynamic modes introduced by each type of interconnection; (ii) the existence of a transition region where phase instability (or chaos) is observed, which makes it possible to detect and store information signals. Estimates of the bistability-region size and of other characteristics of dynamic regimes were obtained in the course of computer simulation; the results suggest that the bistable behavior in the vicinity of the stability-domain boundaries for stable steady-state regimes may constitute one of the general properties of neuronal ensembles with balanced interconnections.

The special features of nonlinear dynamics of the neuronal structures with balanced interconnection under consideration may well be of fundamental importance both for getting insight into the functional capabilities of small nervous systems (like central pacemaking generators) and for the formulation of certain concepts of data processing and storage in large neuronal ensembles. In fact, the temporal characteristics of spikes that are generated by motor neurons of a central pacemaking generator and control the contraction of muscles can vary (owing to bistability and hysteresis) under the effect of a comparatively short-duration stimulus. It is important that such a stimulus fulfills only an informational role—after the stimulation ceases, the system preserves its new state until the next signal arrives. If we keep in mind that, for example, the sensory information is encoded in the interspike spacing, it is easy to conceive the way in which such information can be represented and stored by a neuron ensemble performing the functions considered above. As has been demonstrated quite recently, sensory information (even information that does not exhibit any spatial distribution, e.g., information about odor) is represented by neuron ensembles in the form of spatial patterns [13, 14]. The characteristics of these patterns are defined by the correlation between oscillations of neurons separated spatially, and turn out to be different for dissimilar temporal stimuli. The aforementioned effects related to representation of interspike information in the form of neuron oscillations with differing phase shifts may prove to be useful in developing model concepts of the mechanisms of temporal-pattern

transformation into spatial phase-related structures with simultaneous storage of the latter.

ACKNOWLEDGMENTS

This work was supported by the Russian Foundation for Basic Research (project no. 97-02-17526), the US Department of Energy (grant no. DE-FG03-96ER14592), and the National Science Foundation (grant no. IBN-96334405).

REFERENCES

1. Getting, P.A., *Annu. Rev. Neurosci.*, 1989, vol. 12, pp. 185–204.
2. Steriade, M., McCormick, D.A., and Sejnowski, T.J., *Science* (Washington, DC), 1993, vol. 262, pp. 679–685.
3. *Dynamic Biological Networks: The Stomatogastric Nervous System*, Harrick, R.M., Marder, E., Selverstone, A.I., and Moulins, M., Eds., Cambridge, Mass.: MIT Press, 1992.
4. Selverstone, A.I. and Moulins, M., *The Crustacean Stomatogastric System*, Berlin: Springer-Verlag, 1987.
5. Shepherd, G., *Neurobiology*, Oxford: Oxford Univ. Press, 1983.
6. Abarbanel, H.D.I., Huerta, R., Rabinovich, M.I., Rulkov, N.F., Rowat, P., and Selverstone, A.I., *Neural Computation*, 1996, vol. 8, pp. 1567–1602.
7. Calabrese, R.L., Nadim, F., and Olsen, O.H., *J. Neurobiol.*, 1995, vol. 27, pp. 390–402.
8. Rabinovich, M.I., Selverstone, A., Rubchinsky, L.L., and Huerta, R., *Chaos*, 1996, vol. 6, pp. 288–309.
9. Abarbanel, H.D.I., Rabinovich, M.I., Selverstone, A., Bazhenov, M.V., Huerta, R., Sushchik, M.M., and Rubchinskii, L.L., *Usp. Fiz. Nauk*, 1996, vol. 166, pp. 337–362.
10. Afraimovich, V.S., Verichev, N.N., and Rabinovich, M.I., *Izv. Vyssh. Uchebn. Zaved., Radiofiz.*, 1986, vol. 29, pp. 1050–1060.
11. Huerta, R., Rabinovich, M.I., Abarbanel, H.D.I., and Bazhenov, M.V., *Phys. Rev. E: Stat. Phys., Plasmas, Fluids, Relat. Interdiscip. Top.*, 1997, vol. 55, pp. R2108–R2110.
12. Hindmarsh, J.L. and Rose, R.M., *Proc. R. Soc. London, B*, 1984, vol. 221, pp. 87–102.
13. Wehr, M. and Laurent, G., *Nature* (London), 1996, vol. 384, pp. 162–166.
14. MacLeod, K. and Laurent, G., *Science* (Washington, DC), 1996, vol. 274, pp. 976–979.

Translated by A. Spitsyn